Journal of Geoscience and Environment Protection, 2025, 13(6), 97-117
https://www.scirp.org/journal/gep
ISSN Online: 2327-4344
ISSN Print: 2327-4336

Petrology and Mining Potential of the Niki-Niki Basic to Ultrabasic Massif in Togo, West Africa

Sarakawa Abalo Malibida Kpanzou[1,2*], Koffi Evenyon Kassegne[1], Gnanwasou Alayi[1], Essodina Padaro[1], Kodjo Adika Togbe[1], Mahaman Sani Tairou[1], Yao Agbossoumonde[1], Ouro-Djobo Essoavana Samah[2]

[1]Laboratoire de Géologie, Département de Géologie, Faculté des Sciences, Université de Lomé, Lomé, Togo
[2]Laboratoire de Géotechnique et Mines, Département de Génie Civil, Centre Régional de Formation pour Entretien Routier (CERFER-Conseil de l'Entente), Lomé, Togo
Email: *germalibida@gmail.com

How to cite this paper: Kpanzou, S. A. M., Kassegne, K. E., Alayi, G., Padaro, E., Togbe, K. A., Tairou, M. S., Agbossoumonde, Y., & Samah, O.-D. E. (2025). Petrology and Mining Potential of the Niki-Niki Basic to Ultrabasic Massif in Togo, West Africa. *Journal of Geoscience and Environment Protection, 13,* 97-117.
https://doi.org/10.4236/gep.2025.136008

Received: April 28, 2025
Accepted: June 15, 2025
Published: June 18, 2025

Abstract

The Niki-Niki massif, located in the central part of Togo, belongs to the suture zone of the Pan-African Dahomeyide belt. The aim of this study is to carry out a petrostructural and geochemical investigation of this massif to characterize its associated mining potential. The methodology implemented is based on a summary of previous works, geological mapping, petrographic study of 20 thin sections, geochemical study through discrimination diagrams of 5 rocks samples, and a soil study of a toposequence. The results show that the Niki-Niki massif is composed of garnet-free granulites, pyroxenites and talcschists. Granulites and pyroxenites generally contain plagioclase, clinopyroxene, orthopyroxene and hornblende. Talcschists contain talc, serpentine and chlorite. These parageneses reflect a metamorphic evolution from granulitization to retrograde metamorphism in the amphibolite to green schist facies. Geochemical data show that the rocks of the Niki-Niki massif are metaluminous. They are characterized by enrichment in LREE element relative to HREE elements and display tholeiitic affinity, with negative anomalies in Nb-Ta and Zr. These characteristics suggest a subduction zone magmatism origin. The features are consistent with protoliths of tholeiites, N-MORB and volcanic arc basalts affinities. The Niki-Niki massif rocks were emplaced in an oceanic environment and likely originated from a metasomatized mantle. They offer significant potential for Ni, Cr, Co, V, Cu, Mo and gold (Au) mineralization. These values present a promising target for exploration of these mineral deposits.

Keywords

Geochemistry, Mineral Potential, Niki-Niki Massif, Dahomeyide, Togo

1. Introduction

In the Pan-African Dahomeyide belt, the basic to ultrabasic complexes of Derouvarou (Benin), Kabye-Kpaza, Djabatoure-Anie, Agou-Ahito (Togo), and Shaï or Akuse (Ghana) form a submeridian mountainous belt that marks the suture zone (Ménot et Seddoh, 1980; Agbossoumonde, 1998; Attoh, 1998; Agbossoumonde et al., 2001; Tairou et Affaton, 2013). The Niki-Niki massif, located in the central part of Togo, represents one of the most remarkable morphostructures in this belt. It is defined, like the other massifs of this suture zone, as a metamagmatic ophiolitic-type unit highly metamorphized. The massif is composed of ultramafic, gabbroic metacumulates, metagabbros, metadolerites, metabasalts, pyroxenites, amphibolites and granulites (Ménot, 1977; 1980; 1982; Ménot et Seddoh, 1980; Kassegne, 2017; Kpanzou, 2017; 2023; Kpanzou et al., 2022; 2023a; 2023b). Previous studies (Duclaux, 2003; Sabi, 2007; Agbossoumonde et al., 2007) have partially addressed the petrographic and geochemical characteristics of all the massifs of the Togolese segment of the suture zone. According to these studies, the Niki-Niki massif shows a signature of continental tholeiite emplaced in the continental crust and slow cooling during exhumation. It is also believed that the rocks of the Niki-Niki massif underwent metamorphism in the granulite facies with a retromorphic evolution in the amphibolite facies associated with the overthrust nappes emplacement (Kassegne, 2017; Kpanzou, 2023; Kpanzou et al., 2023a). These are metaluminous rocks with a tholeiitic signature emplaced in a continental or oceanic arc context and exhumed during the Pan-African tangential phase (Tairou, 2006).

Despite efforts to better understand the petrography and geochemistry of the Niki-Niki massif rocks, detailed petrographic and geochemical characterization of these massif rocks remains lacking. Therefore, this study aims to contribute to the detailed petrographic and geochemical understanding of the Niki-Niki massif rocks. Specifically, the goals of this research are to provide 1) a detailed petrographic description of the Niki-Niki massif rocks, 2) a rock classification and origin, 3) a geodynamic environment, and 4) associated mineral occurrences characterization.

2. Geological Setting

The Pan-African Dahomeyide belt resulted from the collision between the eastern portion of the WAC and the Benino-Nigerian basement, representing the south part of the Touareg Shield (Caby et al., 1981; Attoh et al., 1997; Ganade de Araujo et al., 2014). It is subdivided into three structural zones which are from west to east: the external zone, the suture zone and the internal zone (Affaton, 1990) (**Figure 1**).

The external zone corresponds to the Buem and Atacora structural units, composed of metasedimentary rocks originating from the metamorphism of the Volta Basin units, to the orthogneissic units of Kara-Niamtougou and the granitoids complex of Kpalime-Amlame (Affaton, 1990; Affaton et al., 1991; Agbossoumonde et

al., 2007; Tairou et al., 2009; Aidoo et al., 2020; Kwayisi et al., 2021; Tairou et al., 2022; Kwayisi et al., 2024). The external zone overlaps the WAC and its sedimentary cover.

The suture zone is materialized by a submeridian alignment of complexes: Derouvarou in Benin, Kabye-Kpaza, Djabatoure-Anie and Agou-Ahito in Togo, and Akuse or Shaï in Ghana. These complexes are composed of mafic to ultramafic rocks (granulite or sometimes eclogite facies), witnesses of the Pan-African crustal thickening (Ménot & Séddoh, 1985; Attoh, 1998; Agbossoumonde et al., 2001; Attoh & Morgan, 2004; Aidoo et al., 2020; Kpanzou, 2023).

The internal zone is a peneplain representing the remobilized Benin-Nigerian shield (BNS) in the Pan-African belt (Affaton, 1990). It is composed of gneisso-migmatitic, metasedimentary (schists, marbles and quartzites), and Pan-African granitoid units (Affaton et al., 1991; Caby et Boessé, 2001; Alayi, 2018; Alayi et al., 2023).

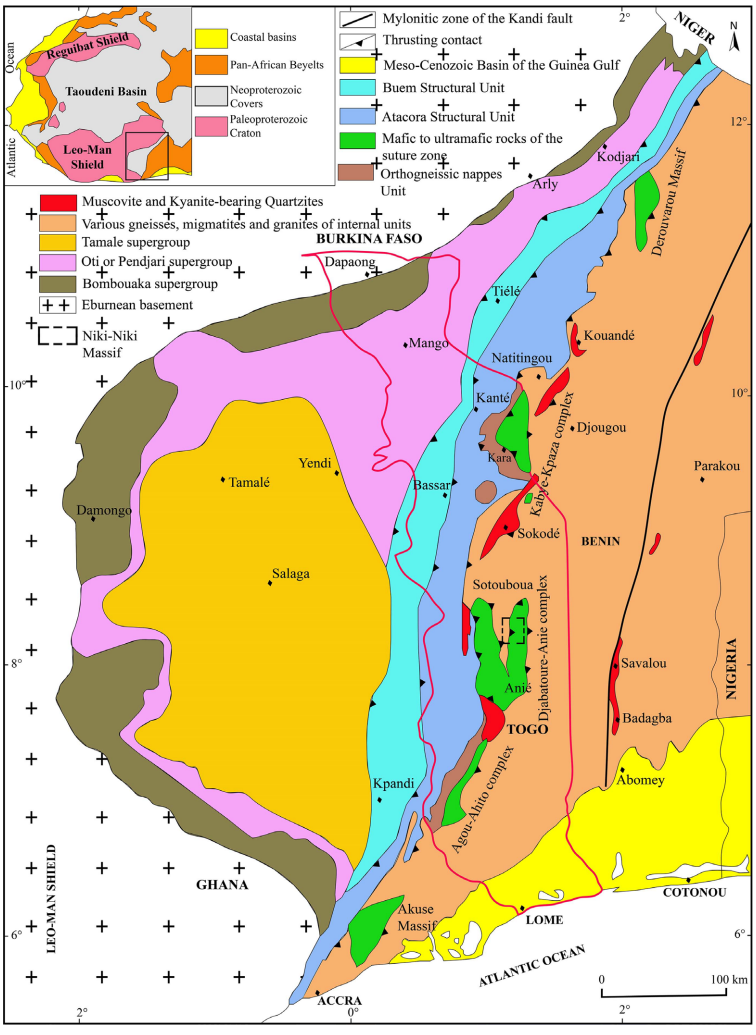

Figure 1. Simplified geologic map showing the main structural domains of the Pan-African Dahomeyide belt and its foreland (Affaton, 1990; slightly modified) with the location of the Niki-Niki massif.

3. Methodology

This study, is based on a literature review of previous work, fieldwork, laboratory analysis, data processing and analysis. The literature review allowed for a synthesis of previous work on the regional and/or local geology of the study area. The field campaign allowed us to take 40 samples and describe their macroscopic petrography. We georeferenced the outcrops and sampling stations using a Garmin eTrex Legend H GPS. Fifteen (15) thin sections were made to determine textural and mineralogical compositions. We selected five (05) samples for whole-rock analysis performed at the Centre for Scientific Instrumentation of the University of Granada (CIC-UGR) in Spain. The analytical approach adopted is as follows:

- Major elements oxides were determined with a Philips Magix Pro (Pw-2440) X-ray fluorescence (XRF) equipment after melting the rock sample in a solution with tetra lithium borate. The characteristic precision as determined from standards AN-G and BEN, was better than ±1.5% (relative error) for an analyte concentration of 10 wt.%. The iron content is expressed as FeO* total. The molar ratio MgO/(MgO + FeO*) is abbreviated Mg#. Zirconium was determined with the same instrument using the same glass beads with a precision better than ±0.2% for 5 ppm Zr. Loss on Ignition (LOI) was determined by weight difference before and after ignition of samples in a furnace. In the diagrams, oxide concentrations are reported in an anhydrous (volatile free) basis.
- Trace elements, except Zr, were determined by an Inductively Coupled Plasma-Mass Spectrometry (ICP-MS) after HNO_3 + HF digestion of 0.1000 g of sample powder in a Teflon-lined vessel at 180˚C and 200 psi for 30 min, evaporation to dryness and subsequent dissolution in 100 ml of 4 vol.% HNO_3; the precision, as determined from standards PMS, WSE, UBN, BEN, BR and AGV run as unknowns, was better than ±2% for analyte concentrations of 50 ppm and ±5% for analyte concentrations of 5 ppm.

The results of the chemical analyses are reported in Table 1. The location of the analyzed samples is shown in Figure 2. Field and chemical data were compiled in Excel and imported into different software (GCD kit, QGIS, …) for specific processing. For the geochemical data processing, we proceeded to the normalization of major elements to 100% under anhydrous basis.

In order to characterize the gold showings, morphological and pedological studies of a toposequence (elementary unit of model) were carried out. This work involved seven (7) prospecting wells and geochemical sampling of the main horizons. The samples collected were subjected to particle size separation by panning. The concentrate obtained was examined under a magnifying glass and visible gold grains were isolated.

4. Results

4.1. Petrography

The Niki-Niki massif (Figure 2) is mainly composed of granulites, pyroxenites and talcschists.

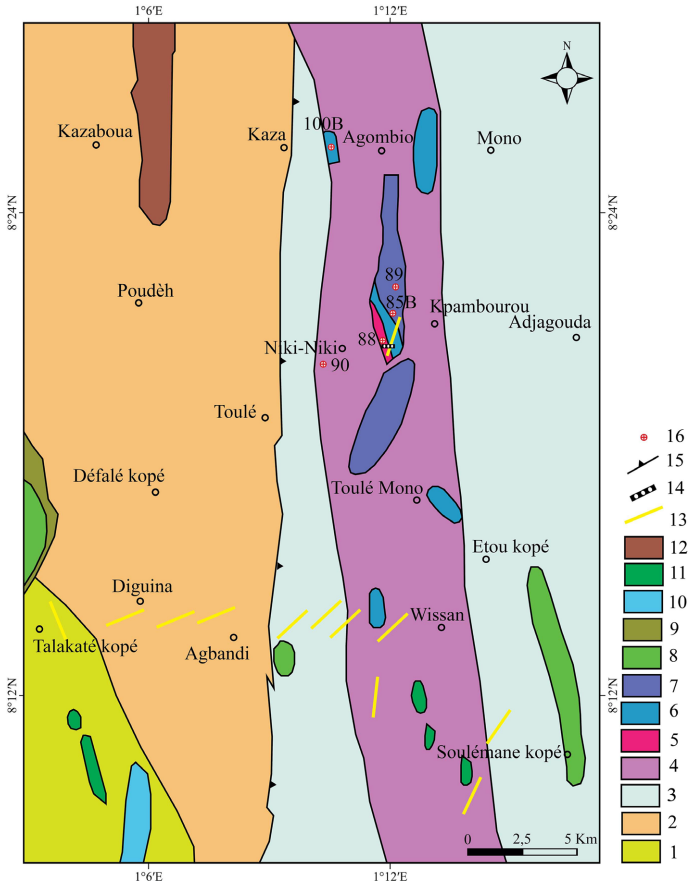

Figure 2. Schematic map of the Niki-Niki massif showing the location of the samples analyzed (modified from the geological map of Sylvain et al., 1986). 1: 2-mica-bearing paragneiss; 2: 2-mica-bearing gneiss; 3: biotite- and amphibole-bearing gneiss; 4: clear metagabbroic granulites; 5: talcschists; 6: pyroxenites; 7: dark metagabbroic granulites; 8: amphibolites; 9: garnet-bearing gneiss; 10: biotite-bearing micaschists; 11: serpentinites; 12: kyanite-bearing gneiss; 13: quartz veins; 14: location of the schematic cross-section; 15: overlapping contact; 16: samples.

4.1.1. Granulites

They are generally garnet-free. They break into milky-white to grayish balls (**Figure 3(a)**). Microscopically (**Figure 3(b)**), they show a granoblastic texture composed of plagioclase, clinopyroxene, and amphibole (green hornblende). Plagioclase is abundant and occurs as phenocrysts with polysynthetic twinning. Clinopyroxene (diopside) are sometimes affected by slightly microfractured or intensely cracked subautomorphic blasts. Amphibole consists of large, elongated, subautomorphic crystals containing oxide inclusions. They are generally very little represented and constitute early minerals in the form of large patches associated with pyroxene. Quartz is fairly rare and occurs in xenomorphic form as inclusion in plagioclase and amphibole.

4.1.2. Pyroxenites

They outcrop in lenses within the granulites. These rocks are often amphibolitized (amphibolo-pyroxenites) and associated with talcschists. These are often cumu-

lating, containing either coarse or fine-grained pyroxene (Figure 3(c)). They are dark gray to black, with a massive structure and a dense spheroidal splitting. Microscopically, they show a granoblastic texture made of clinopyroxene, orthopyroxene, amphibole (green hornblende) and plagioclase (Figure 3(d)). Clinopyroxene (diopside) are lightly colored in green, with numerous cracks and undulatory extinction. Orthopyroxene (hypersthene) is pinkish with undulatory extinction. They are highly cleaved and contain inclusions of opaque minerals (ilmenite, rutile, magnetite). Plagioclase displays phenocrysts with polysynthetic twins and undulatory extinction. Amphibole (green hornblende) appears as elongated phenocrysts joined to pyroxene and plagioclase.

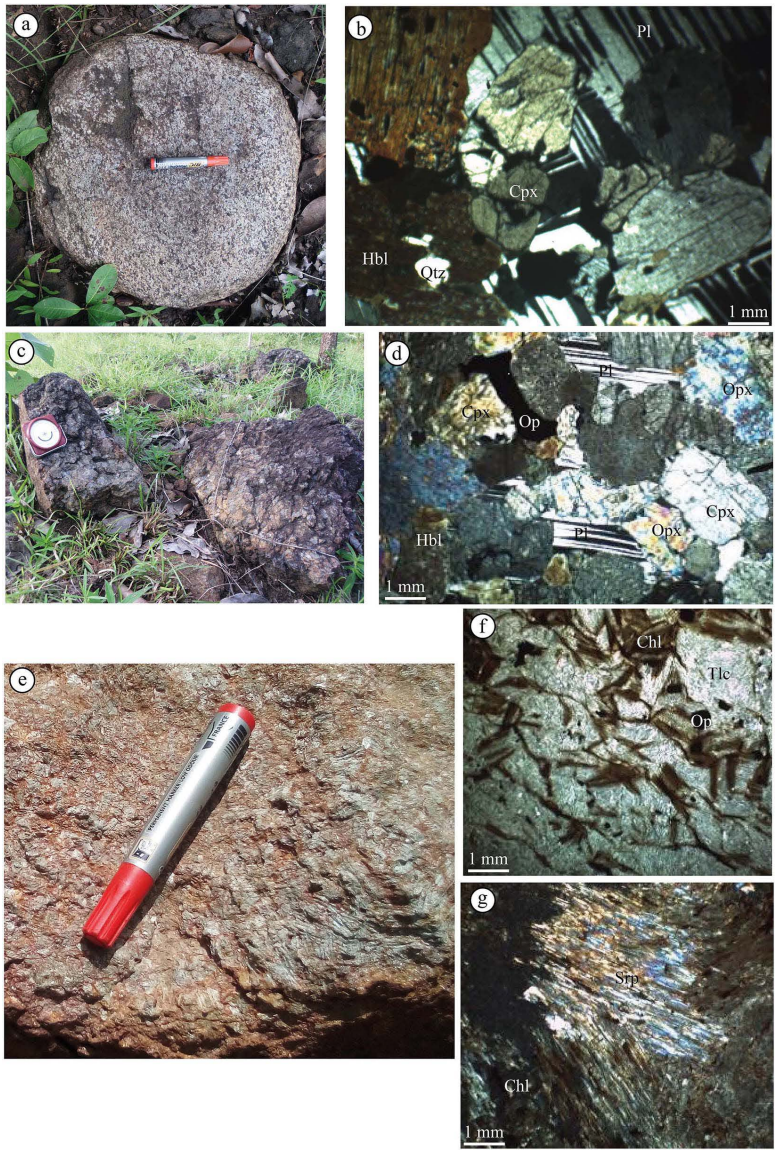

Figure 3. Macroscopic ((a) (c) and (e)) and microscopic ((b) (d) (f) and (g)) photography of the Niki-Niki massif rocks. ((a) and (b)): garnet-free granulite; ((c) and (d)): pyroxenite; ((e) (f) and (g)): talcschist. Opx: orthopyroxene; Cpx: clinopyroxene; Pl: plagioclase; Hbl: hornblende; Srp: serpentine; Chl: chlorite; Tlc: talc; Qtz: quartz; Op: opaque mineral.

4.1.3. Talcschists

They outcrop in balls, laminates or lenses. They are milky white or greenish, with a schistose or laminated structure (Figure 3(e)). Microscopically, they display a lepidoblastic texture with serpentine, talc and chlorite (Figure 3(f) and Figure 3(g)). Serpentine is fibrous and associated with talc, chlorite and opaque minerals (ilmenite, magnetite). Talc appears elongated and spread out. It is often associated with chlorite and derived from retromorphosis of amphibole.

4.2. Geochemistry

4.2.1. Major Elements Distribution

The Niki-Niki massif rocks are characterized by silica contents ranging between 42.45 and 51.86 wt% (Table 1). They are mainly granulites, pyroxenites and talcschists. The analyzed samples show high Al_2O_3 (up to 17.06 wt%) and Sr (up to 580.91 ppm) content, which implies their richness in plagioclase. MgO contents reach 28.72 wt% and Fe_2O_3 up to 14.60 wt% indicating pyroxene cumulate.

According to Harker diagrams (Figure 4), Niki-Niki massif rocks show a positive trend between MgO and FeOt, CaO and a negative trend with SiO_2, TiO_2, Na_2O, K_2O and P_2O_5.

Table 1. Results of geochemical analyses of major elements (wt%), traces elements (ppm) and rare earth elements (ppm) of the Niki-Niki massif rocks.

(a)

Sample	Granulites			Pyroxenite	Talcschist
	85B	89	90	100B	88
Xcoord.	E1˚12'01.9"	E1˚11'51.3"	E1˚10'10.8"	E1˚10'31.1"	E1˚12'03.3"
Ycoord.	N8˚21'12.1"	N8˚21'48.9"	N8˚20'04.1"	N8˚25'33.1"	N8˚21'00.9"
SiO_2 (wt%)	50.64	51.86	49.42	49.1	42.45
Al_2O_3	7.9	17.09	16.6	15.09	2.59
Fe_2O_3	8.74	6.94	10.87	9.00	14.6
MnO	0.15	0.12	0.14	0.15	0.19
MgO	13.76	9.63	6.19	10.9	28.72
CaO	16.05	10.37	9.29	11.87	2.58
Na_2O	0.81	2.51	2.7	1.43	0.11
K_2O	0.16	0.2	0.88	0.33	0.02
TiO_2	0.59	0.38	1.18	0.71	0.24
P_2O_5	0.02	0.04	0.3	0.07	0.02
LOI	0.62	0.45	1.92	0.9	8.09
Total	**99.44**	**99.59**	**99.49**	**99.55**	**99.61**

(b)

Sample	Granulites			Pyroxenite	Talcschist
	85B	89	90	100B	88
Rb (ppm)	4.89	3.29	19.61	5.52	0.65

Continued

Ba	42.72	96.26	240.35	85.92	10.14
Nb	1.14	1.15	2.67	2.26	0.93
Ta	0.08	0.09	0.16	0.14	0.02
Sr	166.39	418.23	580.91	377.78	25.1
Zr	35.5	25,00	90.2	51,00	11.9
Y	19.38	7.89	18.26	14.32	3.74
Hf	1.07	0.28	0.75	0.68	0.07
Ni	359.76	189.36	64.01	150.51	1961.57
Cr	2269.25	363.63	123.63	233.42	2638.46
V	248.01	113.08	304.38	173.92	98.47
U	0.13	0.04	0.17	0.09	0.04
Th	0.00	0.00	0.01	0.00	0.00
Sc	56.84	22.83	26.48	39.15	19.6
Co	60.92	53.13	49.84	60.35	120.63
Cu	123.64	24.76	87.87	119.31	46.86
Zn	49.25	50.18	85.15	66.72	93.21
Mo	1.77	2.84	2.55	2.46	0.76
Cs	0.33	0.24	0.53	0.34	0.15
Li	6.91	5.42	8.72	9.47	0.00
Be	0.3	0.37	0.78	0.4	0.17
Ga	10.13	14.29	20.14	14.38	5.22
Sn	0.37	0.03	0.71	0.35	0.00
Tl	0.04	0.03	0.09	0.04	0.02
Pb	0.65	1.3	3.56	1.68	0.78
La	4.98	3.64	10.67	4.99	1.63
Ce	12.86	7.44	25.12	11.75	3.14
Pr	1.95	1.01	3.51	1.68	0.42
Nd	9.57	4.7	16.24	8.27	2.07
Sm	3.00	1.22	3.89	2.31	0.54
Eu	0.93	0.38	1.29	0.81	0.17
Gd	2.48	1.19	2.94	2.39	0.56
Tb	0.46	0.21	0.46	0.36	0.1
Dy	2.96	1.27	2.85	2.18	0.65
Ho	0.64	0.28	0.6	0.48	0.15
Er	1.64	0.86	1.52	1.31	0.43
Tm	0.24	0.14	0.22	0.2	0.06
Yb	1.43	0.87	1.32	1.17	0.42

Continued

Lu	0.21	0.13	0.19	0.17	0.06
Eu/Eu*	1.02	0.94	1.14	1.03	0.92
(La)N	12.96	9.47	27.78	12.99	4.24
(Sm)N	12.95	5.26	16.79	9.97	2.33
(Gd)N	8.09	3.88	9.59	7.79	1.82
(Yb)N	6.21	3.78	5.73	5.08	1.82
(La/Sm)N	1.00	1.79	1.65	1.30	1.82
(Gd/Yb)N	1.30	1.02	1.67	1.53	1.00
(La/Yb)N	2.08	2.50	4.84	2.55	2.32
ΣREE	43.35	23.34	70.82	38.07	10.4

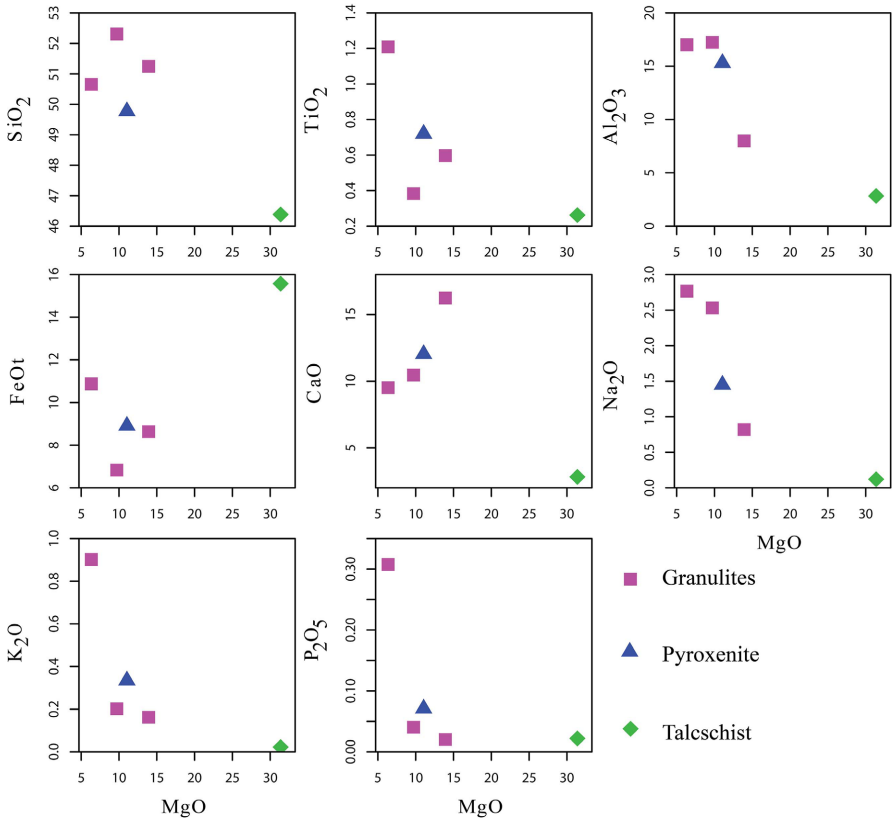

Figure 4. Oxides (SiO_2, FeOt, K_2O, TiO_2, CaO, P_2O_5, Al_2O_3, Na_2O) vs MgO variation diagrams in Niki-Niki massif rocks (Harker, 1909).

4.2.2. Traces and Rare Earth Elements Distribution

In the trace elements (Rb, Y, La, Ba, Ni, Ce, Sr, Cr) versus SiO_2 diagrams (Harker, 1909) (**Figure 5**), Niki-Niki massif rocks show a positive trend between SiO_2 vs Ba, Sr, Y and a negative trend with Ni, Sr, La and Ce.

Chondrite-normalized REE (Nakamura, 1974) (**Figure 6(a)**) and positive mantle normalized spider diagrams (McDonough & Sun, 1995) (**Figure 6(b)**) show that Niki-Niki massif rocks are moderately fractionated ($2.09 \leq (La/Yb)N \leq 4.84$).

They are slightly enriched in LREE ($1 \leq (La/Sm)N \leq 1.82$) and show generally flat heavy rare earth element spectra ($1 \leq (Gd/Yb)N \leq 1.67$). They show slight negative anomalies in Ce, Gd, Dy, Er and positive in Pr, Sm, Ho and Tm.

Primitive mantle normalized spider diagrams (McDonough & Sun, 1995) (**Figure 6(c)**) show that the Niki-Niki massif rocks exhibit negative deplation in Rb, Nb, Ce, Pb, Eu, Ta, Pr, P, Zr, Ti and positive enrichment in Ba, U, La and Pb. The negative Eu anomaly indicates the role of plagioclase during the fractional crystallization processes. The negative anomaly in Nb is characteristic of continental tholeiites and crustal contamination. It suggests that the magmas of these rocks are linked to a plate convergence magmatic environment (subduction zone) where Nb is trapped. The negative anomaly in Ti reflects ilmenite fractionation in these rocks.

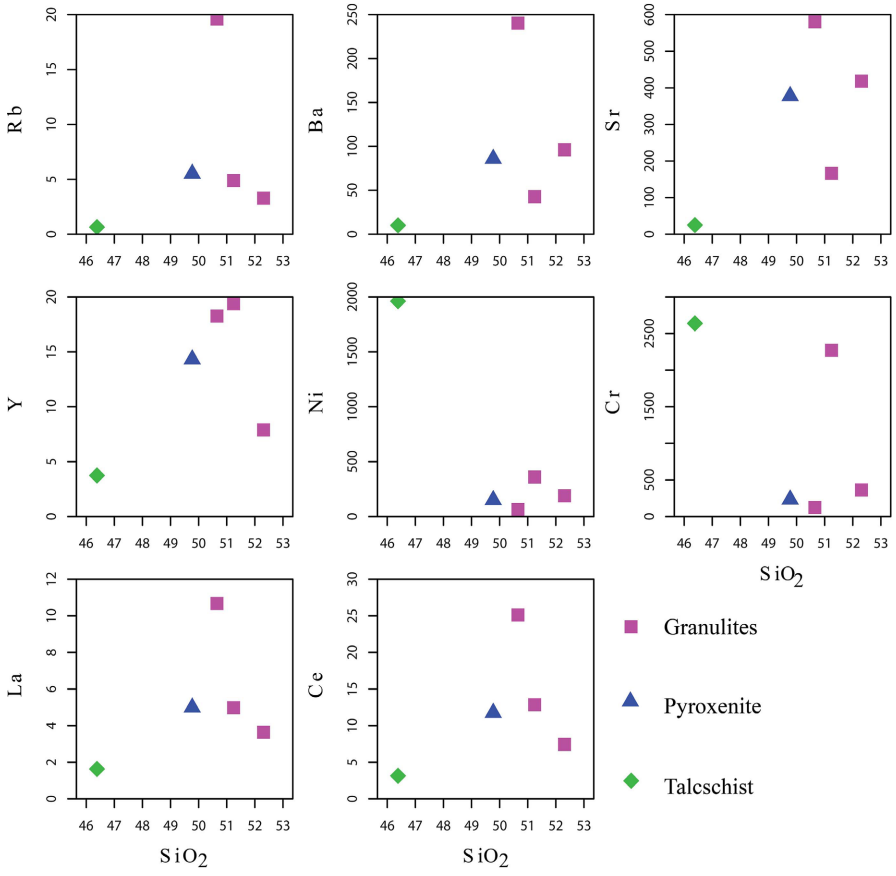

Figure 5. Trace elements (Rb, Y, La, Ba, Ni, Ce, Sr, Cr) versus SiO_2 diagrams in Niki-Niki massif rocks (Harker, 1909).

4.2.3. Type of the Rocks and Geodynamic Context

The rocks of the Niki-Niki massif appear in the TAS diagram of Middlemost (1994) (**Figure 7(a)**) in the gabbros field. The diagram of Irvine & Baragar (1971) (**Figure 7(b)**) indicates that these rocks show tholeiitic affinity. The diagram of Foley et al., (1987) and Shand (1943) (**Figure 7(c)**) shows that these rocks are meta- to peraluminous. The diagram of Meschede (1986) (**Figure 7(d)**) shows that the

rocks of the Niki-Niki massif are distributed in the N-MORB (D) and intraplate tholeiitic and volcanic arc basalts (C) fields.

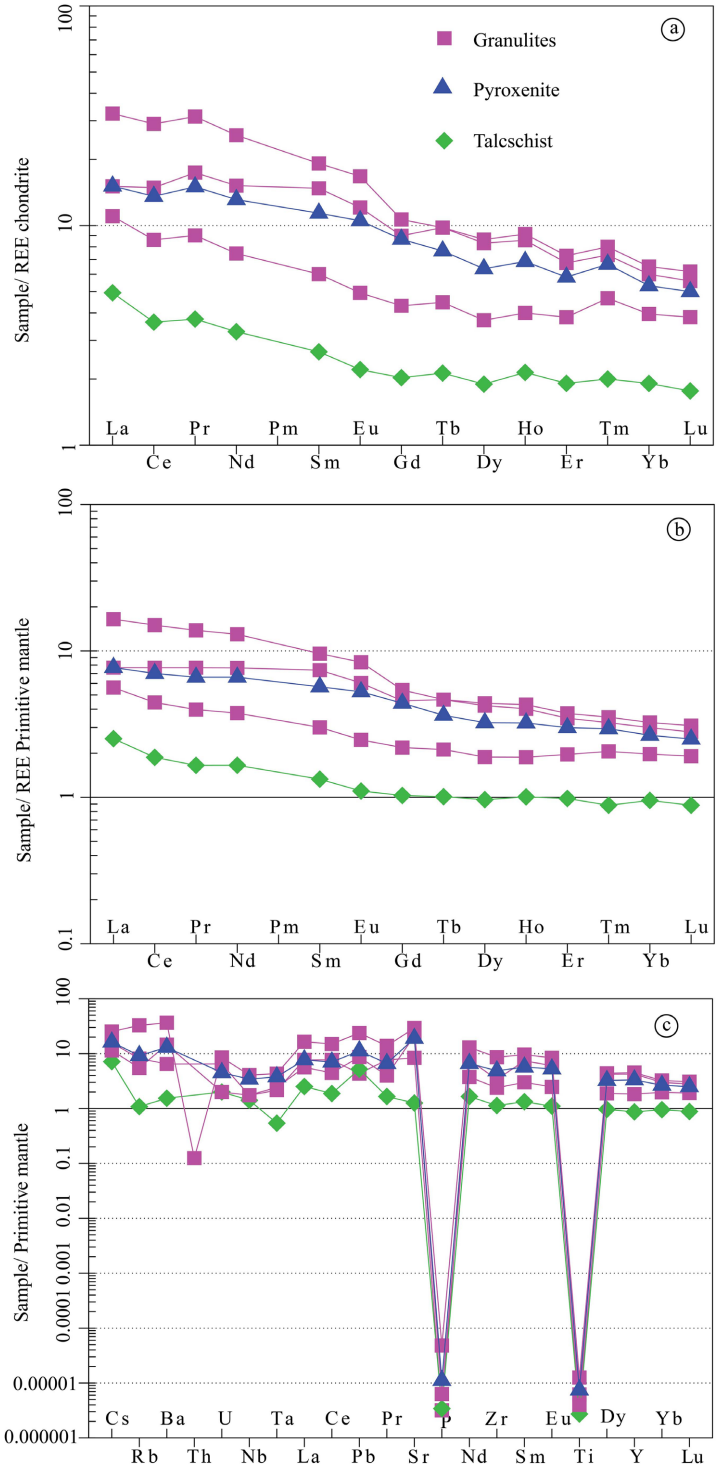

Figure 6. (a) Rare earth elements spectra normalized to chondrites (Nakamura, 1974), (b) trace elements spectra normalized to the primitive mantle (McDonough et Sun, 1995) and (c) primitive mantle normalized spider diagrams (McDonough et Sun, 1995) of the Niki-Niki massif rocks.

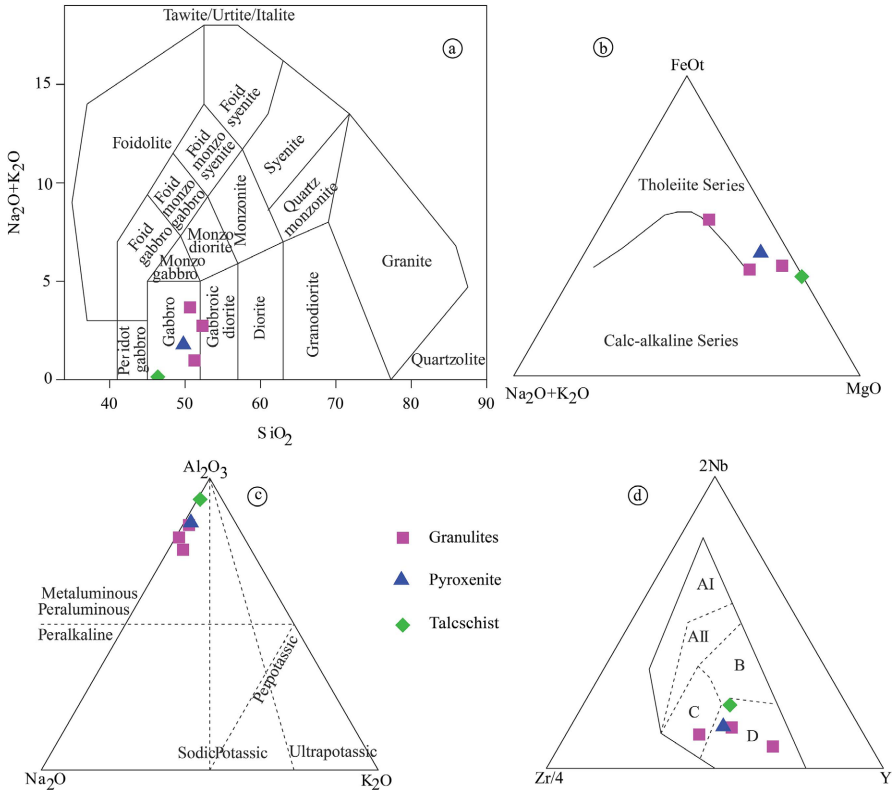

Figure 7. Geochemical classification plots of Niki-Niki massif showing the type (a), magmatic affinities ((b) and (c)) and geotectonic context (d) of rocks. (a): $Na_2O + K_2O$ vs SiO_2 (Middlemost, 1994); (b): FeOt-($Na_2O + K_2O$)-MgO (Irvine & Baragar, 1971); (c): Na_2O-Al_2O_3-K_2O (mol%) (Foley et al., 1987) and peraluminosity (Shand, 1943); (d): Zr/4-Nb-Y (Meschede, 1986) [AI = intraplate alkaline basalts; AII = intraplate alkaline basalts and tholeiites; B = E-type MORB; C = intraplate tholeiites and volcanic arc basalts; D = N-type MORB].

4.3. Mineralization

4.3.1. Base Metals Potential

Geochemical results on whole rock (**Table 1**) and field observations reveal the presence of significant anomalies for some of the base metals; notably chromium, nickel, vanadium, copper and cobalt (**Figure 8**). Chromium anomalies range from 123 ppm to 2638 ppm; nickel anomalies range from 64 ppm to 1961 ppm (**Figure 8**).

4.3.2. Gold Potential

Among the seven prospecting wells, the NP5 located on the western slope of the Niki-Niki massif (X = 301,579 E, Y = 923,101 N, H = 296 m) showed significant gold showings along the toposequence (**Figure 9**). It has a depth of 220 cm. Its profile consists of four horizons, from top to bottom: gravelly soil, ferruginous crust, gravel horizon, silty horizon (**Figure 10(a)**).

- gravelly soil (from 0 cm to 10 cm)

This is a thin horizon of soil made up of dark-red ferruginous gravel, exhibiting a lumpy structure and a sandy-clay loam texture. The fragments are sub-rounded and the entire layer is powdery, interspersed with numerous rootlets.

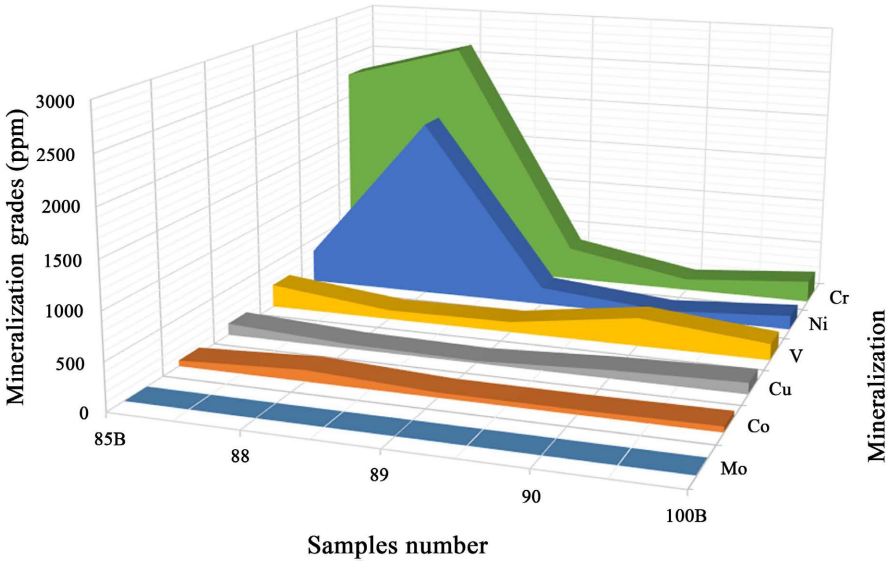

Figure 8. Signatures of the base metals (Ni-Cr-V-Cu-Co-Mo) of the rocks of the Niki-Niki massif.

- ferruginous crust (from 10 cm to 100 cm)

This horizon has a compact structure and a silty-clay texture with numerous ferruginous gravels (Figure 10(b)). These ferruginous nodules form an indurated horizon. The strong cohesion between the ferruginous nodules indicates extensive leaching. The nodules have a black core and an ochre-red periphery. In addition to these nodules, there are a few angular quartz fragments.

- gravelly horizon (from 100 cm to 150 cm)

It consists of angular quartz pebbles loosely bound by a brick-red clay matrix. The pebbles range from centimetric to decimetric in size and are believed to have originated from the disintegration of a quartz vein located 10 meters east of shaft NP5. A panning test carried out on an excavated sample of angular gravel revealed the presence of gold (0.1 to 2 mm in size) (Figure 10(c)).

- lithomarge (from 150 cm to 220 cm)

This horizon is clearly distinct from the gravelly horizon. It consists essentially of brick-red clay with the same macroscopic characteristics as the clay matrix of the overlying horizon. The few ferruginous gravels observed are softer and can be broken easily with the fingers. This horizon has a lumpy structure and a clayey texture.

5. Discussion

5.1. Petrography and Metamorphic Evolution

The petrographic study of the Niki-Niki massif reveals a diversity of facies: granulites, pyroxenites and talcschists. Granulites are generally garnet-free with a mineralogical assemblage of Pl + Cpx + Opx + Hbl. Amphibolitization has led to granulites transformation into amphibolites characterized by Hbl + Pl + Qtz paragenesis, indicating a transition from granulite to amphibolite facies. Pyroxenites

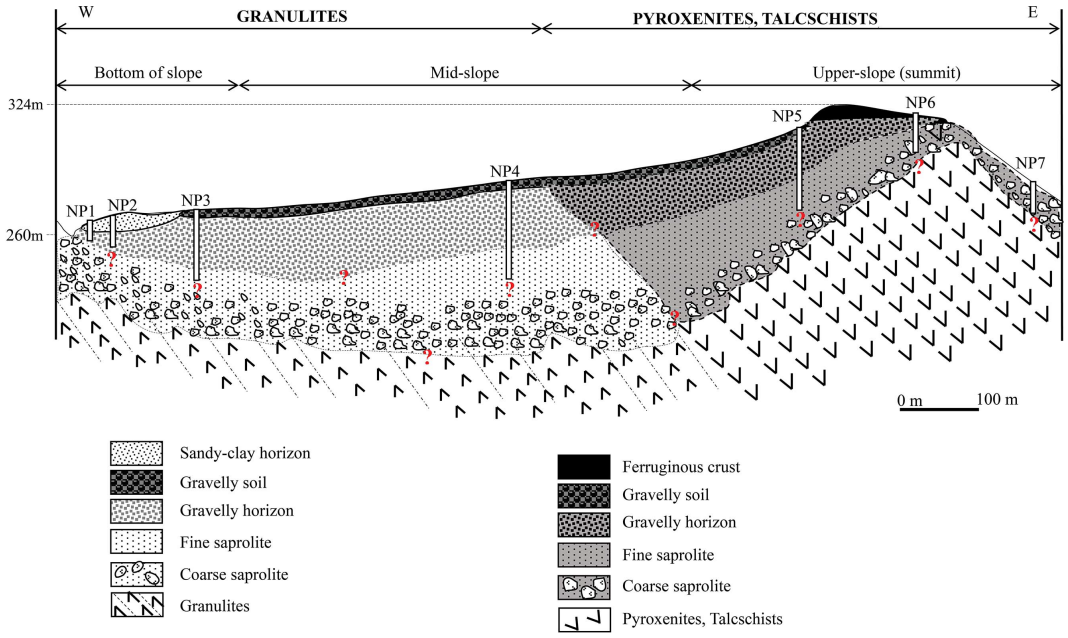

Figure 9. Schematic cross-section of sampled toposequence (question marks indicate extrapolated limits; depths are expressed in centimeters).

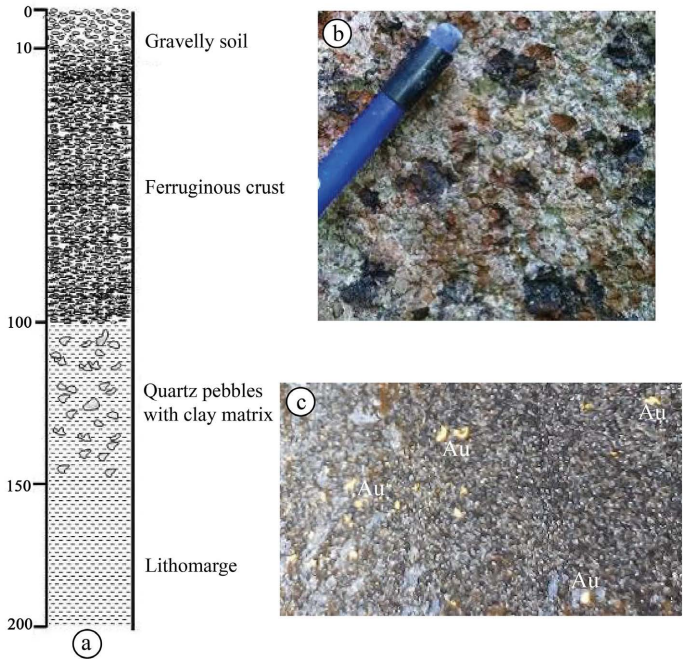

Figure 10. (a): Weathering profile; (b) Accumulation horizon textures; (c): Gold powder; Au: gold.

have an Opx + Cpx + Pl + Hbl paragenesis and underwent an initial retrograde metamorphism in the amphibolite facies, where pyroxenes were replaced by green hornblende. Talcschists show a paragenesis of Tlc + Srp + Chl, with the appearance of talc and chlorite marking the transition to greenschist facies. These paragenesis and metamorphic conditions are similar to those in the Kabye, Agou and

Akuse massifs (Agbossoumonde, 1998; Agbossoumonde et al., 2001; Attoh & Morgan, 2004; Sabi, 2007).

5.2. Fractional Crystallization

The correlations observed in the Harker variation diagrams for major and trace elements, and the parallelism of the rare earth and multi-element spectra, suggest that the different facies evolved from a single magmatic source.

The slight negative anomalies in Nb-Ta reflect the crustal recycling influence (crustal contamination). The positive anomaly in Sr suggests plagioclase accumulation. The good linear correlation in the Harker diagrams reflects the role of fractional crystallization in the differentiation process during the evolution of the parent magmas of these massif rocks (Agbossoumonde, 1998; Agbossoumonde et al., 2001; Sabi, 2007).

The increase in FeOt versus MgO reflects the crystallization of pyroxene and amphibole. The decrease in TiO_2 and P_2O_5 versus MgO suggests the fractional crystallization of ilmenite and apatite. The decrease in Na_2O and K_2O reflects the enrichment of these rocks in acidic plagioclase (Tairou et al., 2022; Guillot et al., 2019; Kpanzou, 2023).

The increase in Ba content suggests the high fractionation of plagioclase in these rocks. The decrease in Ni and Cr contents versus SiO_2 indicates the fractionation of ferromagnesian (pyroxene and amphibole) of these rocks. These elements could also be associated with MgO and FeOt in pyroxenes according to some authors (Hamlaoui et al., 2020; Kpanzou, 2023).

5.3. Source of Magmas

The rocks of the Niki-Niki massif have a basic to ultrabasic composition. Their chemical characteristics allow us to classify them as gabbros according to Middlemost (1994) terminology. Petrographic characteristics reflect the chemical composition of these rocks with abundant hornblende and the presence of orthopyroxene and clinopyroxene. Negative anomalies in elements such as niobium, phosphorus and titanium, observed in multi-element spectra, are signature features typically associated with subduction zone magmas. The negative anomaly in Nb is characteristic of continental tholeiites and suggests crustal contamination or metasomatism from a mantle source (Kpanzou et al., 2022; Kpanzou, 2023; Kpanzou et al., 2023a; 2023b).

The genesis of these rocks is therefore compatible with emplacement in a magmatic arc context with simultaneous crustal assimilation and fractional crystallization of magma probably derived from continental crust.

5.4. Geotectonic Environment

Based on the petrogeochemical data of the Niki-Niki massif rocks, such as their tholeiitic affinity and meta- to peraluminous signature, it can be proposed that they were emplaced in a probably extensive tectonic context like most of basic to

ultrabasic massifs of the Pan-African suture zone (Duclaux, 2003; Guillot et al., 2019; Kpanzou et al., 2022).

Geotectonic discrimination diagrams indicate that these rocks are emplaced in various settings: N-MORB, intraplate tholeiites and volcanic arc basalts. The negative anomaly in Nb is characteristic of continental tholeiites and crustal contamination. It suggests a context of subduction zone in which Nb is trapped (Guillot et al., 2019; Kpanzou et al., 2022; Kpanzou, 2023).

The geochemical characteristics of the Niki-Niki massif rocks are similar to those of the Kabye, Agou and Djabatoure massifs rocks, such as high Sr and Ba values, a negative anomaly in Nb, and enrichment in light rare earth elements (LREE) compared to heavy rare earth elements (HREE) (Affaton, 1990; Agbossoumonde, 1998; Duclaux, 2003; Sabi, 2007; Kpanzou, 2023, Kpanzou et al., 2023a). These rocks have also been subsequently contaminated by continental crust.

Despite the lack of isotopic data, petrogeochemical studies of the Niki-Niki massif rocks show similarities with those of the Kabye, Agou, Akuse and Djabatoure massifs, allowing to classify them in the same geodynamic context.

5.5. Mineralization Indices

The highest content of Ni (359 to 1961 ppm) and Cr (2269 to 2638 ppm) are well above the average for common basaltic fluids, which range from 200 to 300 ppm for Ni and 400 to 500 ppm for Cr (Bougault et al., 1980).

The concentrations of Ni (1961 ppm), Cr (2638 ppm), Cu (123 ppm), V (304 ppm), Co (120 ppm) and Mo (2 ppm) are also higher than the average values for the Earth's crust, which are Ni (105 ppm), Cr (185 ppm), Cu (75 ppm), V (230 ppm), Co (29 ppm), and Mo (1 ppm) (Taylor & McLennan, 1985, 1995). Similarly, the strategic prospecting work carried out by BRGM (Dempster, 1967) also revealed concentrations of Au (1000 ppb), Cu (341 ppm), Cr (3053 ppm), Ni (2104 ppm), V (136 ppm) and Mo (20 ppm). The results of the current research confirm the existence of these mineral occurrences in the study area.

Gold showings in one of the shafts dug along the toposequence (**Figure 9**) further corroborate BRGM's findings, which indicated that gold panning occurs near outcrops of galena quartz veins (Picot et al., 1989). The presence of these crushed quartz veins indicates a shear zone which is often associated with mineralization, represented here by the gold powder collected.

The gold dust and anomalous base metal values found in the study area represent an important target for exploration of these mineral occurrences.

6. Conclusion

Petrographic studies of the Niki-Niki massif have identified: granulites, pyroxenites and talcschists. The mineralogies of these rocks are dominated by a primary paragenesis consisting of an abundance of plagioclase, followed by clinopyroxene. A secondary paragenesis is mainly represented by alteration minerals such as amphibole, chlorite and talc. These parageneses show that these rocks underwent

metamorphism in the granulite facies, with retrogression in the amphibolite to green schist facies. Thus, the massif has undergone a metamorphic evolution from granulitization to retrograde metamorphism in the amphibolite to green schist facies.

Geochemical characterization shows that the Niki-Niki massif rocks are meta- to peraluminous and have a tholeiitic affinity. Inter-element variations indicate that these rocks evolved from a fractional crystallization process accompanied by crustal contamination. They were emplaced in various settings: N-MORB, intraplate tholeiites and volcanic arc basalts. They are crustal base rocks uplifted by Pan-African tectonics in crustal sets. Geochemical trends clearly indicate their emplacement in a subduction context.

The Niki-Niki massif rocks show enrichment in light rare earth elements (LREE) compared to heavy rare earth elements (HREE), with sub-flat HREE spectra. Multi-element spectra shows that most rocks are rich in mobile elements (Ba) and have negative anomalies in Nb-Ta, P and Ti. These characteristics are similar to those of rocks derived from a mantle source that was enriched and metasomatized during a subduction event.

In terms of mineralization, the area is characterized by gold, chromium, and potentially nickel occurrences.

Acknowledgements

I would like to express my gratitude to the universities of the Coimbra Group who, through the "Coimbra Group Short Stay Scholarship Programme for young researchers from Sub-Saharan Africa", have granted me a laboratory research scholarship for the realization of geochemical analyses of rock samples. I also extend thanks Professors Antonio Garcia-Casco and José María González-Jiménez, both professors-researchers at the Department of Petrology and Mineralogy of the University of Granada in Spain, for their support of my scholarship application and for carrying out the chemical analyses of my rock samples in their laboratory. Lastly, we acknowledge the anonymous reviewers for their constructive feedback, which significantly enhanced the quality of the initial manuscript.

Conflicts of Interest

This article presents no conflict of interest, and the authors wish to have the work published in this journal.

References

Affaton, P. (1990). *Le bassin des Volta (Afrique de l'Ouest): Une marge passive d'âge protérozoïque supérieur, tectonisée au Panafricain (600 ± 50 Ma)* (500 p.). ORSTOM, Collection Etudes & Thèses. https://horizon.documentation.ird.fr/exl-doc/pleins_textes/pleins_textes_2/etudes_theses/31718.pdf

Affaton, P., Gelard, J. P., & Simpara, N. (1991). Paléocontraintes enregistrées par la fracturation dans l'unité structurale de l'Atacora (Chaîne Panafricaine des Dahomeyides,

Togo). *Comptes rendus de l'Académie des Sciences, Paris, 312,* 763-768. https://pascal-francis.inist.fr/vibad/index.php?action=getRecordDetail&idt=19679359

Agbossoumonde, Y. (1998). *Les complexes ultrabasiques de la chaîne panafricaine au To-go (Axe Agou-Atakpamé, Sud-Togo). Etude pétrographique, minéralogique et géochimique* (306 p.). Thèse Doct. Lab. Géol. Pétro. Univ. Jean Monnet St. Etienne Fr.

Agbossoumonde, Y., Menot, R., & Guillot, S. (2001). Metamorphic Evolution of Neoproterozoic Eclogites from South Togo (West Africa). *Journal of African Earth Sciences, 33,* 227-244. https://doi.org/10.1016/s0899-5362(01)80061-0

Agbossoumondé, Y., Ménot, R., Paquette, J. L., Guillot, S., Yéssoufou, S., & Perrache, C. (2007). Petrological and Geochronological Constraints on the Origin of the Palimé-Amlamé Granitoids (South Togo, West Africa): A Segment of the West African Craton Paleoproterozoic Margin Reactivated during the Pan-African Collision. *Gondwana Research, 12,* 476-488. https://doi.org/10.1016/j.gr.2007.01.004

Aidoo, F., Sun, F., Liang, T., & Nude, P. M. (2020). New Insight into the Dahomeyide Belt of Southeastern Ghana, West Africa: Evidence of Arc-Continental Collision and Neoarchaean Crustal Reworking. *Precambrian Research, 347,* Article ID: 105836. https://doi.org/10.1016/j.precamres.2020.105836

Alayi, G. (2018). *Les granitoïdes tardifs de la chaîne panafricaine des Dahomeyides au Togo: Étude pétro-structurale, géochimique et géochronologique* (256 p.). Thèse Doctorat, FDS, Univ. Lomé-Togo.

Alayi, G., Kpanzou, S. A. M., Agbossoumondé, Y., Padaro, E., Menot, R., & Tairou, M. S. (2023). Petrology, Age and Geodynamic Implication of the Pan-African Granitoids Associated with the Glito-Kpatala Shear Zone (South-East Togo). *International Journal of Geosciences, 14,* 1193-1225. https://doi.org/10.4236/ijg.2023.1412061

Attoh, K. (1998). High-Pressure Granulite Facies Metamorphism in the Pan-African Dahomeyide Orogen, West Africa. *The Journal of Geology, 106,* 236-246. https://doi.org/10.1086/516019

Attoh, K., & Morgan, J. (2004). Geochemistry of High-Pressure Granulites from the Pan-African Dahomeyide Orogen, West Africa: Constraints on the Origin and Composition of the Lower Crust. *Journal of African Earth Sciences, 39,* 201-208. https://doi.org/10.1016/j.jafrearsci.2004.07.048

Attoh, K., Dallmeyer, R. D., & Affaton, P. (1997). Chronology of Nappe Assembly in the Pan-African Dahomeyide Orogen, West Africa: Evidence from Mineral Ages. *Precambrian Research, 82,* 153-171. https://doi.org/10.1016/s0301-9268(96)00031-9

Bougault, H., Joron, J. L., & Treuil, M. (1980). The Primordial Chondritic Nature and Large-Scale Heterogeneities in the Mantle: Evidence from High and Low Partition Coefficient Elements in Oceanic Basalts. *Philosophical Transactions of the Royal Society A, 297,* 63-114.

Caby, R., & Boessé, J. M. (2001). Pan-African Nappe System in Southwest Nigeria: The Ife-Ilesha Schist Belt. *Journal of African Earth Sciences, 33,* 211-225. https://doi.org/10.1016/s0899-5362(01)80060-9

Caby, R., Bertrand, J. M., & Black, R. (1981). Pan-African Closure and Continental Collision in the Hoggariforas Segment, Central Sahara. In A. Kröner (Ed.), *Precambrian Plate Tectonics* (pp. 407-443). Elsevier. https://www.scirp.org/%28S%28351jmbntvnsjt1aadkozje%29%29/reference/referencespapers.aspx?referenceid=1160492

Dempster, A. N. (1967). *Prospecting and Evaluation of the Agbandi Region, Togo* (22 p.).

Duclaux, G. (2003). *Etude pétrologique et structurale des massifs basiques et ultrabasiques*

de la zone de suture panafricaine de la chaîne des Dahomeyides au Togo: Implications géodynamiques (29 p.). Mém. DEA, Lab. Dyn. Lithos. Univ. J. Monnet, St-Etienne. https://doi.org/10.13140/RG.2.2.28332.92809

Foley, S. F., Venturelli, G., Green, D. H., & Toscani, L. (1987). The Ultrapotassic Rocks: Characteristics, Classification, and Constraints for Petrogenetic Models. *Earth-Science Reviews, 24,* 81-134. https://doi.org/10.1016/0012-8252(87)90001-8

Ganade de Araujo, C. E., Rubatto, D., Hermann, J., Cordani, U. G., Caby, R., & Basei, M. A. S. (2014). Ediacaran 2,500-km-Long Synchronous Deep Continental Subduction in the West Gondwana Orogen. *Nature Communications, 5,* Article No. 5198. https://doi.org/10.1038/ncomms6198

Guillot, S., Agbossoumondé, Y., Bascou, J., Berger, J., Duclaux, G., Hilairet, N. et al. (2019). Transition from Subduction to Collision Recorded in the Pan-African Arc Complexes (Mali to Ghana). *Precambrian Research, 320,* 261-280. https://doi.org/10.1016/j.precamres.2018.11.007

Hamlaoui, H., Laouar, R., Bouhlel, S., & Boyce, A. J. (2020). Caractéristiques pétrologiques et géochimiques des roches magmatiques d'El Aouana, NE algérien. *Estudios Geológicos, 76,* e124. https://doi.org/10.3989/egeol.43391.510

Harker, A. (1909). *The Natural History of Igneous Rocks* (384 p.). Cambridge University Press. https://doi.org/10.1017/cbo9780511920424

Irvine, T. N., & Baragar, W. R. A. (1971). A Guide to the Chemical Classification of the Common Volcanic Rocks. *Canadian Journal of Earth Sciences, 8,* 523-548. https://doi.org/10.1139/e71-055

Kassegne, K. E. (2017). *Etude d'une toposéquence pédologique issue des métapyroxénites amphibolitisées et métagabbros à Niki-Niki (Préfecture de Blitta)* (50 p.). Mém. Master, FDS, Univ. Lomé.

Kpanzou, S. A. M. (2017). *Etude pétrographique et structurale du massif de Djabatouré et des massifs adjacents* (31 p.). Mém. Master, FDS, Univ. Lomé.

Kpanzou, S. A. M. (2023). *Contribution à l'étude du complexe basique-ultrabasique de Djabatouré-Anié (Centre-Togo): Caractéristiques pétrostructurales, géochimiques et indices de minéralisations associés* (232 p.). Thèse de Doctorat unique, Univ. Lomé.

Kpanzou, S. A. M., Agbossoumonde, Y., González Jiménez, J. M., Tairou, M. S., & Garcia-Casco, A. (2022). Pétrologie et métallogénie des indices de Ni-Cr associés au massif basique-ultrabasique de Oké, Togo. *Afrique SCIENCE, 21,* 53-69. https://www.afriquescience.net/article.php?nid=448&&code=Vol.21,%20N%C2%B01%20(2022)&id=5

Kpanzou, S. A. M., Alayi, G., Agbossoumondé, Y., Tairou, M. S., González-Jiménez, J. M., & Garcia-Casco, A. (2023a). Petrographic and Geochemical Characteristics of the Djabatoure Massif Metamagmatites from the Pan-African Orogen in Central Togo, West Africa. *European Scientific Journal, ESJ, 19,* 198. https://doi.org/10.19044/esj.2023.v19n24p198

Kpanzou, S. A. M., Alayi, G., Tairou, M. S., & Agbossoumonde, Y. (2023b). Petrographic and Geochemical Characteristics of the Akaba Igneous Massif from the Pan-African Orogen in Togo, West Africa. *Journal of Environment and Earth Science, 13,* 18-30. https://doi.org/10.7176/JEES/13-7-03

Kwayisi, D., Amponsah, P. O., Agra, N. A., Nunoo, S., Thompson, J., Kazapoe, R. W. et al. (2024). Neoproterozoic Passive Margin Formation and Evolution during the Rodinia Gondwana Supercontinent Cycle at the Eastern Margin of the West African Craton. *Geological Magazine, 161,* e14. https://doi.org/10.1017/s001675682400027x

Kwayisi, D., Elburg, M., & Lehmann, J. (2021). Preserved Ancient Oceanic Lithosphere

within the Buem Structural Unit at the Eastern Margin of the West African Craton. *Lithos, 410,* Article ID: 106585. https://doi.org/10.1016/j.lithos.2021.106585

McDonough, W. F., & Sun, S. (1995). The Composition of the Earth. *Chemical Geology, 120,* 223-253. https://doi.org/10.1016/0009-2541(94)00140-4

Menot, R. P. (1980). Les massifs basiques et ultrabasiques de la zone mobile pan-africaine au Ghana, Togo et Benin; etat de la question. *Bulletin de la Société Géologique de France, 7,* 297-303. https://doi.org/10.2113/gssgfbull.s7-xxii.3.297

Ménot, R., & Seddoh, K. F. (1985). The Eclogites of the Lato Hills, South Togo, West Africa: Relics from the Early Tectonometamorphic Evolution of the Pan-African Orogeny. *Chemical Geology, 50,* 313-330. https://doi.org/10.1016/0009-2541(85)90126-3

Ménot, R.-P. (1977). *Les massifs basiques et ultrabasiques antémétamorphiques de la bordure Ouest du mole Dahoméo-nigérian. Essai de synthèse bibliographique* (pp. 53-94). Ann. Univ. Bénin. https://www.researchgate.net/publication/327822999

Ménot, R.-P. (1982). Les éclogites des Monts Lato: Un témoin de l'évolution tec-tono-métamorphique de la chaîne pan-africaine du Togo (Afrique de l'Ouest). *Docum. Lab. Géol. Lyon*, n° 87, 63 p. https://www.persee.fr/doc/geoly_0750-6635_1982_num_87_1_1513

Ménot, R.-P., & Seddoh, K. F. (1980). Le massif basique stratifié précambrien de Djabatoure-Soutouboua (région centrale du Togo, Afrique de l'Ouest). Pétrologie et évolution métamorphique. *Bulletin du B.R.G.M., 4,* 319-337. https://www.researchgate.net/publication/260887781

Meschede, M. (1986). A Method of Discriminating between Different Types of Mid-Ocean Ridge Basalts and Continental Tholeiites with the Nb-Zr-Y Diagram. *Chemical Geology, 56,* 207-218. https://doi.org/10.1016/0009-2541(86)90004-5

Middlemost, E. A. K. (1994). Naming Materials in the Magma/Igneous Rock System. *Earth-Science Reviews, 37,* 215-224. https://doi.org/10.1016/0012-8252(94)90029-9

Nakamura, N. (1974). Determination of REE, Ba, Fe, Mg, Na and K in Carbonaceous and Ordinary Chondrites. *Geochimica et Cosmochimica Acta, 38,* 757-775. https://doi.org/10.1016/0016-7037(74)90149-5

Picot, J. C., Aissah, J. C., Coste, B., Godonou, K. S., & Joannes, C. (1989). *Prospection minière stratégique entre les 8ème et 10ème parallèles* (150 p.). Rapport BRGM 89 TGO 165.

Sabi, B. E. (2007). *Etude pétrologique et structurale du Massif Kabyè, Nord-Togo* (256 p.). Thèse Doctorat, Univ. Lomé.

Shand, S. J. (1943). *Eruptive Rocks. Their Genesis, Composition, Classification and Their Relations to Ore Deposits* (2nd ed., 444 p.) Murby. https://www.scirp.org/(S(czeh2tfqyw2orz553k1w0r45))/reference/ReferencesPapers.aspx?ReferenceID=1945539

Sylvain, J. P., Collart, J., Aregba, A., & Godonou, S. (1986). *Notice explicative de la carte géologique 1/500.0000è du Togo, Mém.* n°6, D.G.M.G./B.N.R.M., Lomé-Togo.

Tairou, M. S. (2006). *La tectonique tangentielle panafricaine au Nord-Togo* (399 p). Thèse de Doctorat, Univ. Lomé.

Tairou, M. S., & Affaton, P. (2013). Structural Organization and Tectono-Metamorphic Evolution of the Pan-African Suture Zone: Case of the Kabye and Kpaza Massifs in the Dahomeyide Orogen in Northern Togo (West Africa). *International Journal of Geosciences, 4,* 166-182. https://doi.org/10.4236/ijg.2013.41015

Tairou, M. S., Affaton, P., & Sabi, B. E. (2009). Tectono-Metamorphic Evolution of the Mo and Kara-Niamtougou Orthogneic Suites, Northern Togo. *Global Journal of Geological*

Sciences, 7, 93-100. https://www.researchgate.net/publication/287411921

Tairou, M. S., Miningou, Y. M. W., Costa, Y. D. D., & Kwekam, M. (2022). Petrostructural and Geochemical Characteristics of the Metamagmatites in the External Zone of the Dahomeyides Belt: Case of the Kantè Serpentinites (Northern Togo). *International Journal of Geosciences, 13,* 779-792. https://doi.org/10.4236/ijg.2022.139039

Taylor, S. R., & McLennan, S. M. (1985). *The Continental Crust: Its Composition and Evolution*. Blackwell Scientific Publishers.

Taylor, S. R., & McLennan, S. M. (1995). The Geochemical Evolution of the Continental Crust. *Reviews of Geophysics, 33,* 241-265. https://doi.org/10.1029/95rg00262